UNIVERSITA' DEGLI STUDI DI TRENTO
Department of Industrial Engineering

Laboratory activity – Properties and Characterisation of materials (module 1)

Evaluation of fracture properties of polymeric materials: resistance to crack propagation and impact conditions.

Professor: Dorigato Andrea
Lab. Assistant: Rigotti Daniele

Students:

Arduini Giacomo (Matr.[redacted])
Cresci Alex (Matr.[redacted])
Leso Sergio Maria (Matr.[redacted])
Pascolo Gaia (Matr.[redacted])

A.Y. 2020-2021

Contents

1 Introduction

In the second part of the laboratory activity the aim is to study the fracture toughness of Poly(methyl methacrylate) (PMMA) and the influence of the specimen thickness. PMMA is an amorphous thermoplastic polymer. It presents a glass transition temperature around 105 °C. PMMA is commonly known as Plexiglass and is used as a shatter resistant alternative to glass due to its transparency. In this sense it can compete with Polycarbonate (PC) when tensile and flexural strength are the main deciding factors. Acrylic bone cement typically consists of PMMA with some filler materials and is used in orthopedics to fix both the femoral and acetabular components in a total hip replacement. Today, in most total joint replacements including the hip, knee, and ankle, acrylic bone cement is used as a means of fixation of the prosthesis to the bone. Bone cement is also often used in the fixation of pathological fractures and in the repair of bone defects[1].
Fracture toughness is a critical mechanical property for engineering applications. For brittle and semi-brittle materials, predominantly linear-elastic (LEFM) conditions are assumed. This means low toughness and little to no plastic deformation occurring at the crack tip. Fracture toughness is quantified by the stress intensity factor K_C and is a measure of the resistance of a material to crack extension. K_C can be used to relate the critical stress for crack propagation to the crack length on engineering components. The test performed on single edge notched bend specimens (SEN-B test) is based LEFM theory and is consists of a three point flexure test using a prenotched specimen. The test is sensitive to a variety of factors such as the notch-sharpening technique[2]and the specimen thickness, since bigger dimensions allow for a larger number of defects in the material and may potentially decrease the fracture toughness measured.

Another aim is to study the impact behaviour of glass fibre reinforced polypropylene and in particular the dependence on the notch radius of curvature. Polypropylene (PP) is a semi-crystalline polymer widely used in industry for its low cost and excellent processability. It is possible to add fibres to the polymeric matrix in order to increase mechanical properties. Glass fibers (GF) are the most common reinforcement for polymeric matrix composites. Their principal advantages are the relationship between their low cost, high tensile strength, high chemical resistance, and insulating properties. The disadvantages are low tensile modulus, relatively high specific gravity, sensitivity to abrasion during handling, low fatigue resistance, and high hardness[3].
Charpy impact testing is a cheap yet reliable method to study the fracture behavior and impact strength of materials. It is commonly required for construction codes, especially for fracture-critical structures such as bridges and pressure vessels. However, the method is highly sensitive to changes in test parameters such as impact velocity, specimen geometry and shape, and that's why it is used to analyse the impact behaviour as function of the notch radius[4].

2 Materials and methods

2.1 Fracture toughness

2.1.1 Specimens description and measurement

Fracture toughness test was performed on single edge notched bend specimens made of Poly(methyl methacrylate) (PMMA). Two samples of 3 specimens each were tested. The first sample (specimens A, B, and C) was obtained from a 15 mm thick PMMA sheet. The second sample (specimens D, E and F) was obtained from a 10 mm thick sheet. This allowed for the investigation of the thickness effect on the fracture toughness values. The dimensions of the specimens such as $width\ (W)$ and $thickness\ (B)$ were measured with a digital caliper and repeated three times to allow for some statistical significance. The fracture surface was observed under an optical microscope and the $pre-crack\ length\ (a)$ was measured three times using the Imagej software. The average dimensions of the specimens are reported in table 2.1.

Specimens	Average W $[mm]$	Average B $[mm]$	Average a $[mm]$
A	15.26 ± 0.02	7.969 ± 0.006	6.25 ± 0.08
B	15.08 ± 0.03	7.798 ± 0.006	6.50 ± 0.09
C	15.03 ± 0.06	7.903 ± 0.007	6.73 ± 0.03
D	10.285 ± 0.006	4.979 ± 0.002	4.74 ± 0.02
E	10.253 ± 0.007	4.990 ± 0.004	5.01 ± 0.02
F	10.26 ± 0.04	5.09 ± 0.02	5.63 ± 0.01

Table 2.1: Average dimensions of the cross section and pre-crack length of the specimens.

2.1.2 Description of the test

The test was performed according to the ASTM D5045[5] standard, consisting of a 3 point flexure test performed on SEN-B specimens. The instrument utilized was an Instron 5969 with a load cell of 50 kN. The span length (S) for the specimens was set to four times the width (corresponding to 60 mm for the A,B and C specimens and to 40 mm for the D, E and F specimens). The test speed was 10 $mm\ min^{-1}$. A scheme of the bending rig is shown in Figure 2.1.

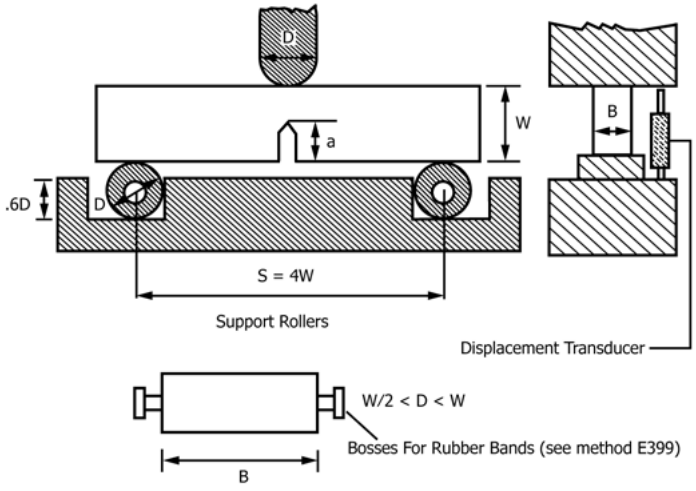

Figure 2.1: Bending rig with transducer for SEN-B.

2.1.3 Parameters of the test

The test aimed to investigate the fracture toughness in plane strain conditions of the specimens, or K_{IC}. A trial value of fracture toughness can be calculated as follows:

$$K_Q = (\frac{P_Q}{BW^{1/2}})f(x) \tag{2.1}$$

Where:

$$f(a/W) = 6(x)^{1/2}\frac{[1.99 - x(1-x)(2.15 - 3.93x + 2.7x^2)]}{(1+2x)(1-x)^{3/2}} \tag{2.2}$$

and

$$0 < x = \frac{a}{W} < 1 \tag{2.3}$$

The trial K_Q values are taken to be valid K_{IC} values if they pass the size check assuring that plain strain conditions are respected and the plasticity in the crack tip is not excessive.
The critical strain energy release rate in plain strain conditions G_{IC} was calculated. A trial calculation can be obtained as:

$$G_Q = \frac{U}{BW\varphi}, \tag{2.4}$$

where U represents the corrected energy. The corrected energy (U) is calculated as follows:

$$U = U_Q - U_i, \tag{2.5}$$

where U_Q represents the energy derived from integration of the load versus displacement curve up to the same load point as used for K_{IC}. This energy must be corrected for the system compliance, loading-pin penetration, and specimen compression. This can be done by subtracting the integrated energy of a load-displacement curve of an indentation test (U_i) performed at the same parameters of the SEN-B test. The parameter φ is the energy calibration factor and can be computed from the following:

$$\varphi = \frac{A + 18.64}{dA/dx} \tag{2.6}$$

where:

$$A = [16x^2/(1-x)^2][8.9 - 33.717x + 79.616x^2 - 112.952x^3 + 84.815x^4 - 25.672x^5] \tag{2.7}$$

$$dA/dx = [16x^2/(1-x)^2][-33.717+159.232x-338.856x^2+339.26x^3-128.36x^4] \\ +[32x/(1-x)^3][8.9-33.717x+79.616x^2-112.952x^3+84.815x^4-25.672x^5] \tag{2.8}$$

2.1.4 Validity checks

In order for the test to be compliant with the ASTM D5045[5] standard, the specimens must first pass a dimension check, ensuring that:

$$0.45 < \frac{a}{W} < 0.55 \tag{2.9}$$

The test is conducted assuming LEFM and plain strain conditions. For this reason, the geometry of the specimen must be such that plasticity in the crack tip is not excessive, and that the thickness B is sufficiently high. As B becomes bigger than the crack dimension, the fracture toughness K_C becomes independent of thickness. This requirements can be summarized in the following criterion:

$$B, a, (W-a) > 2.5(K_Q/\sigma_Y)^2, \tag{2.10}$$

Each load vs. displacement curve must respect a linearity requirement. An example of load vs. displacement curve is represented in Figure 2.2. The compliance C of the specimen is defined as $tan(\theta)$, where θ is the angle between the vertical axis and the linear part of the curve (AB). A line (AB') is drawn such that the new inverse of the slope is $tan(\theta') = 1.05C$. The maximum load of the curve is defined as P_{MAX}. The criterion to be respected is:

$$P_{MAX}/P_Q < 1.1 \tag{2.11}$$

If P_{MAX} is comprised between AB and AB', P_Q is taken to be equal to P_{MAX}. If P_{MAX} is at the right of AB', the load corresponding to the intercept between the curve and AB' is defined as P_Q.

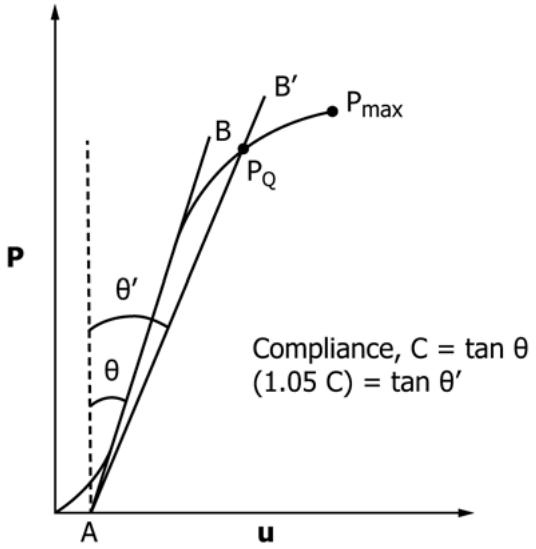

Figure 2.2: Linearity check.

In order to roughly evaluate the goodness of the results, a relationship can be used to calculate Young's modulus from K_{IC}, G_{IC} and the Poisson's ratio (ν). The modulus can be confronted with typical values of the investigated material:

$$E = \frac{(1-\nu^2)K_{IC}^2}{G_{IC}}. \tag{2.12}$$

2.2 Impact test

2.2.1 Specimens description and measurement

Charpy impact test was performed on Polypropylene (PP) samples reinforced with glass fibres (25%wt). The impact loading is a severe testing case, the high deformation rate makes the material more brittle and decreases its toughness.
Specimens for the test were obtained by producing notches with different radius of curvature (1 *mm*, 0.25 *mm*, 0.1 *mm*, and 0.01 *mm*) in the middle. In order to do this, different razor blades were used. In this way a triaxial state of stress is introduced. For each radius of curvature two specimens were obtained and for each specimen three measurements of the cross-section dimensions were done in order to have some statistical data. The average dimensions of the specimens are reported in Table 3.1.

Specimens	Notch radius $[mm]$	Average thickness $[mm]$	Average width $[mm]$
A	1	3.98 ± 0.01	9.91 ± 0.01
B	1	3.97 ± 0.01	9.90 ± 0.01
C	0.25	3.99 ± 0.02	9.88 ± 0.03
D	0.25	3.99 ± 0.01	9.90 ± 0.01
E	0.1	3.98 ± 0.01	9.88 ± 0.01
F	0.1	3.98 ± 0.01	9.89 ± 0.01
G	0.01	3.98 ± 0.01	9.91 ± 0.01
H	0.01	3.98 ± 0.01	9.89 ± 0.03

Table 2.2: Average dimensions of the cross section of the specimens.

For the test, the standard ASTM D6110[6] was followed.

2.2.2 Description of the test

The apparatus was composed by a pendulum Ceast and a hammer Ceast M544 (weight 2.5 *kg*, length 0.325 *m*), the starting angle was of 69°. A pivoting arm is raised to a specific height (in order to have a constant potential energy) and then released. The arm swings down hitting the notched specimen and transferring a percentage of its initial energy to break it. An example of how the machine works is shown in Figure 2.3.

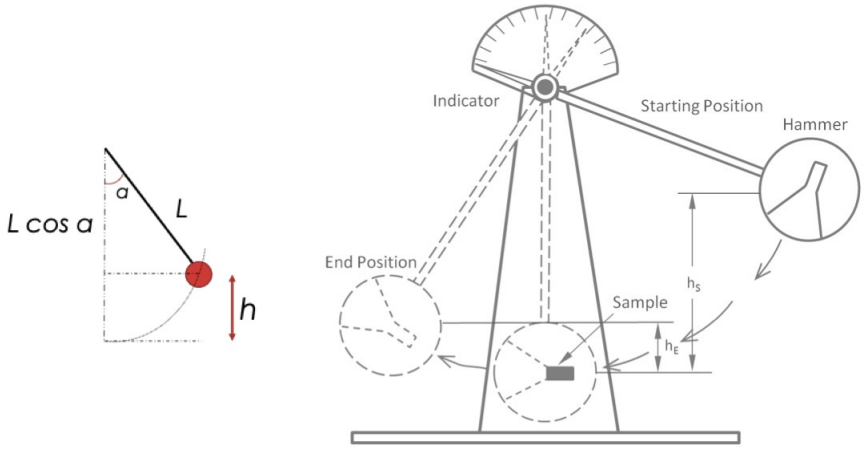

Figure 2.3: Charpy test scheme.

2.2.3 Parameters of the test

The initial energy can be calculated as:

$$E = mgh = 5.4\,J, \tag{2.13}$$

where m is the mass of the hammer, g is the gravity constant and h is the height of the pivoting arm. Thanks to the instrumented test (tup strain gage), it is possible to monitor the evolution of the force the specimen is subjected to, as function of the time, the frequency of acquisition was 2kHz. It is important to consider that vibrations induced by the impact process in the sensor and in the specimen can produce some inertial effects. To avoid this problem it is possible to use plasticine dampening between the machine and the specimen.
Plotting the force as function of the displacement it is possible to obtain the absorbed energy as the integral of the curve:

$$\Delta U = v_0 \int_0^t F dt - \frac{1}{2m}\left[\int_0^t F dt\right]^2 \tag{2.14}$$

In order to calculate the displacement, the initial height and the final velocity must be determined. Making reference to the scheme in Figure 2.3:

$$h = L(1 - cos(\alpha)) \tag{2.15}$$

$$t = \sqrt{\frac{2h}{g}} \tag{2.16}$$

$$v = gt \tag{2.17}$$

Since the test is very fast and the material behaves in a brittle manner, it is possible to neglect the energy loss and take this velocity to calculate the displacement as:

$$Displacement = vt \tag{2.18}$$

As last step, the specific absorbed energy can be determined by dividing the calculated absorbed energy by the cross section in correspondence of the region where the impact occurs, and hence by subtracting the notch length to the original width of the specimen to obtain the real width of the cross-section.

3 Results and discussion

3.1 Fracture toughness

The results of the fracture toughness tests are shown in Figures from 3.1 to 3.2, where the load is plotted against the displacement.

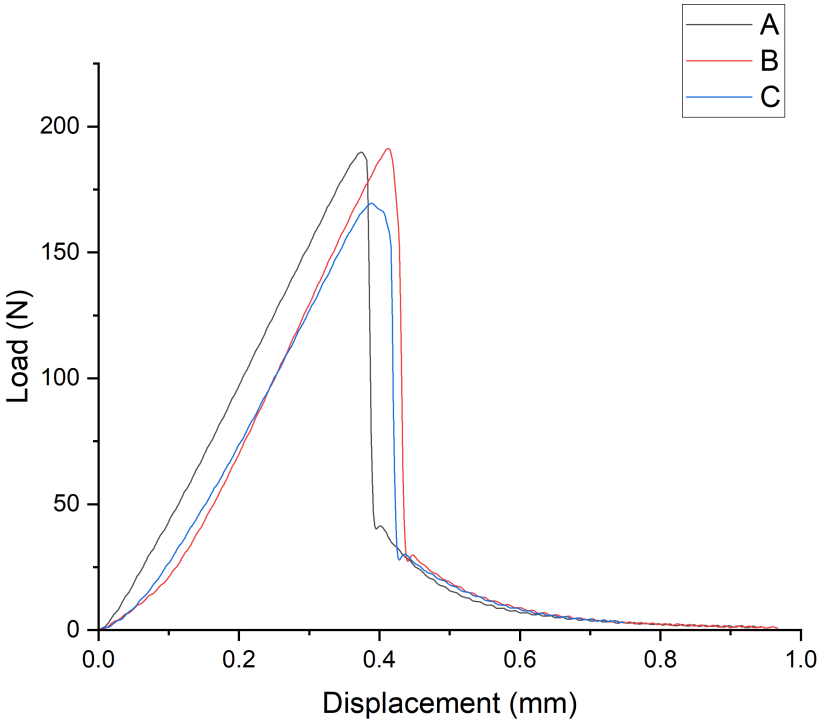

Figure 3.1: Results of the fracture toughness test performed on specimens A, B and C.

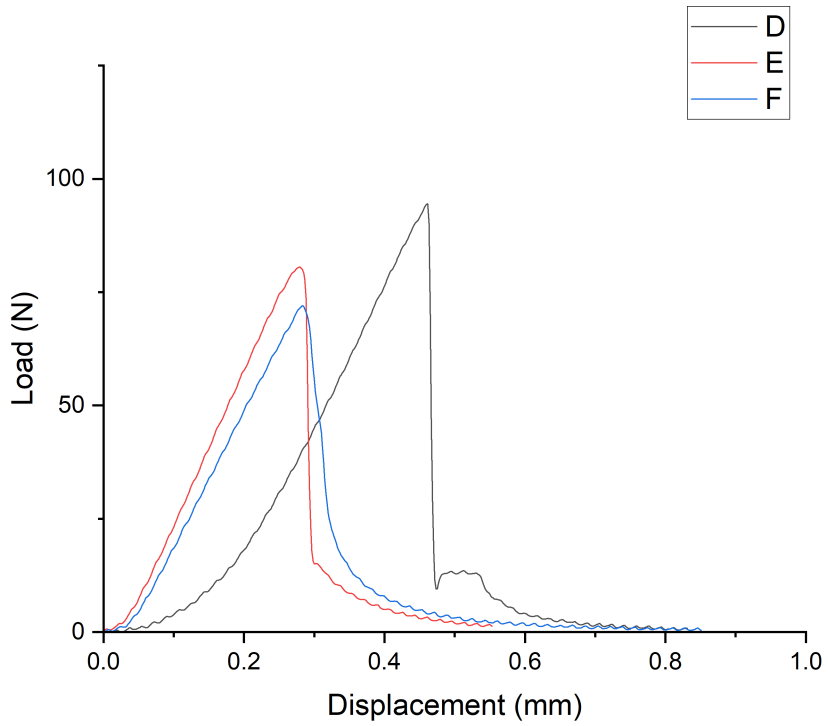

Figure 3.2: Results of the fracture toughness test performed on specimens D, E and F.

The results of the indentation tests for the specimens A and D are shown in Figure 3.3 and 3.4.

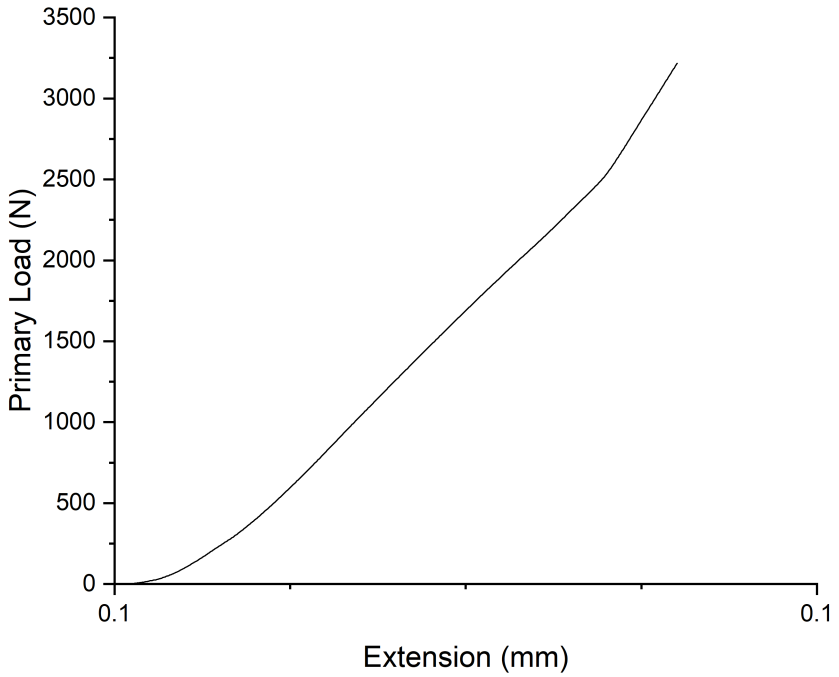

Figure 3.3: Results of the indentation test performed on specimen A.

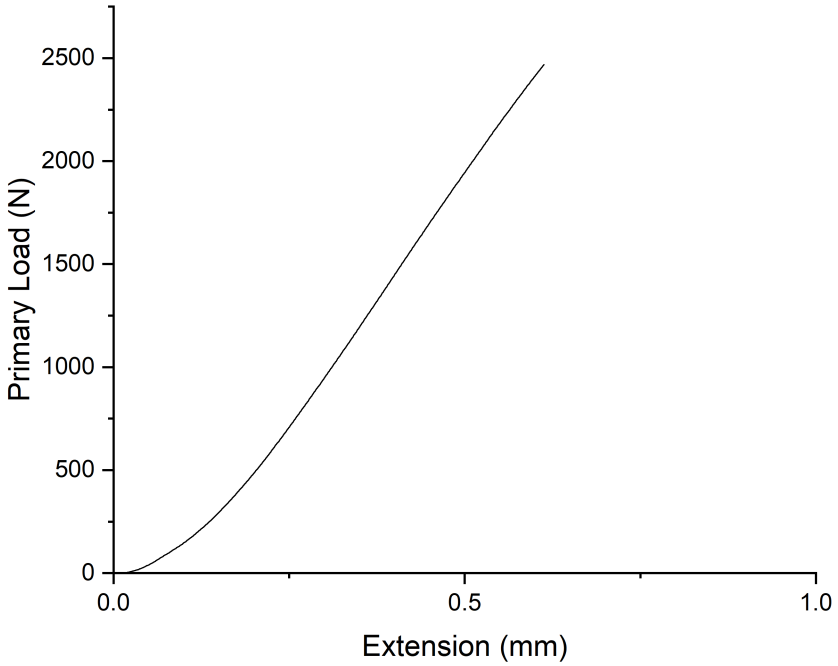

Figure 3.4: Results of the indentation test performed on specimen D.

The first three specimens (A, B, C) don't pass the dimension check, with a a/W ratio below the desired mark. However, the experimental results pass the remaining validity checks. The fracture toughness curves all respect the linearity requirements. The values of K_{IC}, G_{IC} and E are reported on table .

Specimens	K_{IC} $[MPa\sqrt{m}]$	G_{IC} $[kJ/m^2]$	E [GPa]
A	$1.568880 \pm 3x10^{-6}$	0.738 ± 0.001	2.853 ± 0.005
B	$1.728045 \pm 3x10^{-6}$	0.776 ± 0.002	3.294 ± 0.007
C	$1.588221 \pm 3x10^{-6}$	0.711 ± 0.003	3.04 ± 0.01
D	$1.767304 \pm 3x10^{-6}$	0.9588 ± 0.0007	2.787 ± 0.002
E	$1.639655 \pm 3x10^{-6}$	0.6914 ± 0.0007	3.327 ± 0.003
F	$1.746829 \pm 2x10^{-6}$	0.671 ± 0.004	3.89 ± 0.02

Table 3.1: Calculated values of K_{IC}, G_{IC} and E of the specimens.

The specimens all pass the size check, showing that the initial hypothesis of brittle material and LEFM condition is correct. The fracture toughness and critical strain energy release rate can be considered as calculated in plane strain condition. In Figures 3.5 and 3.6, K_{IC} and G_{IC} are represented in red for the larger (from 15 mm sheet) specimens and in blue for the smaller (from 10 mm sheet) specimens.

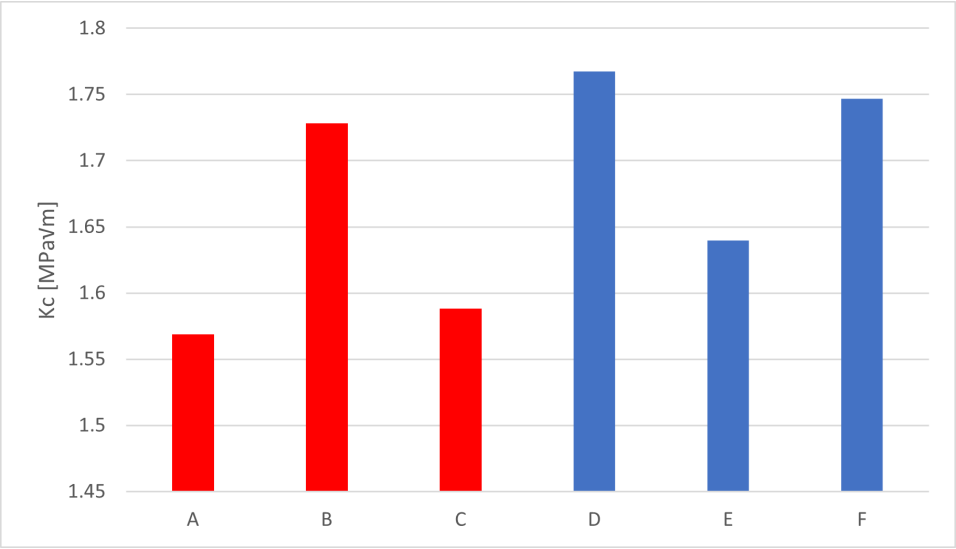

Figure 3.5: Fracture toughness (K_{IC}) of the specimens grouped by size.

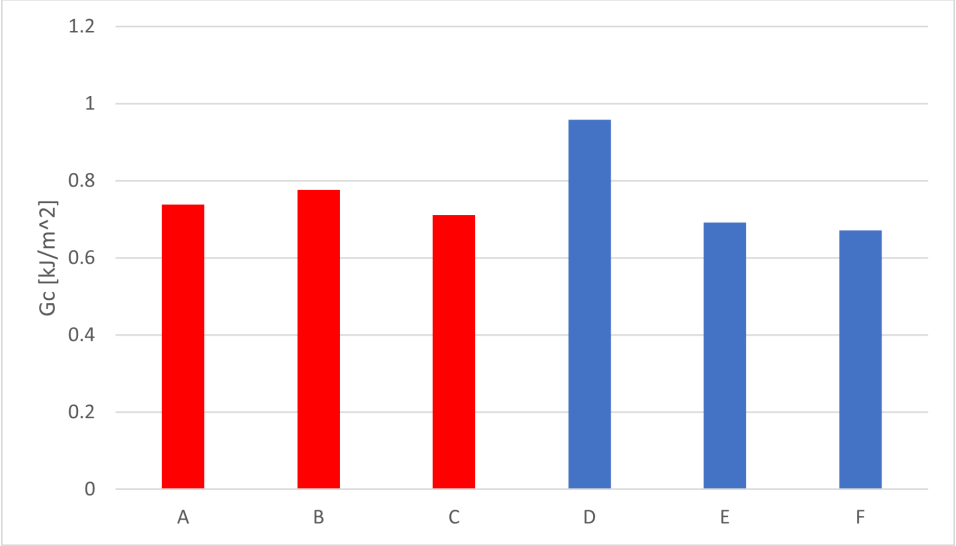

Figure 3.6: Critical strain energy release rate (G_{IC}) of the specimens grouped by size.

The average fracture toughness for the smaller specimens was slightly higher ($1.72 \pm 0.06\ MPa\sqrt{m}$) in respect to the larger specimens ($1.63 \pm 0.07\ MPa\sqrt{m}$), a difference of 5.5%. The small sample size however results in a large error and casts doubts on the validity of the obtained result. A similar consideration can be done for the critical strain energy release rate. For the smaller specimens the average value was higher ($0.8 \pm 0.1\ kJ/m^2$) in comparison to the larger specimens ($0.74 \pm 0.03\ kJ/m^2$), a difference of 4.4%. This however can be solely attributed to one of the specimen (D) having a particularly large G_{IC} value, and also in this case the small sample size results in a significant error. The size effect on K_{IC} and G_{IC} remains unclear.

3.2 Impact test

The results of the impact test are shown in Figures from 3.7 to 3.10, where the load is plotted as function of time.

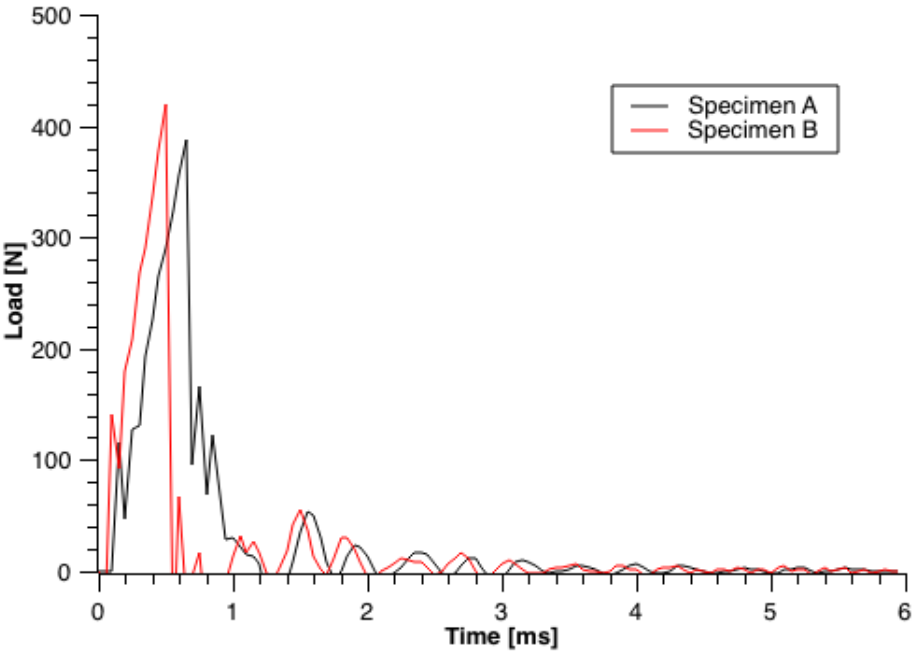

Figure 3.7: Results of the impact test performed on specimens A and B.

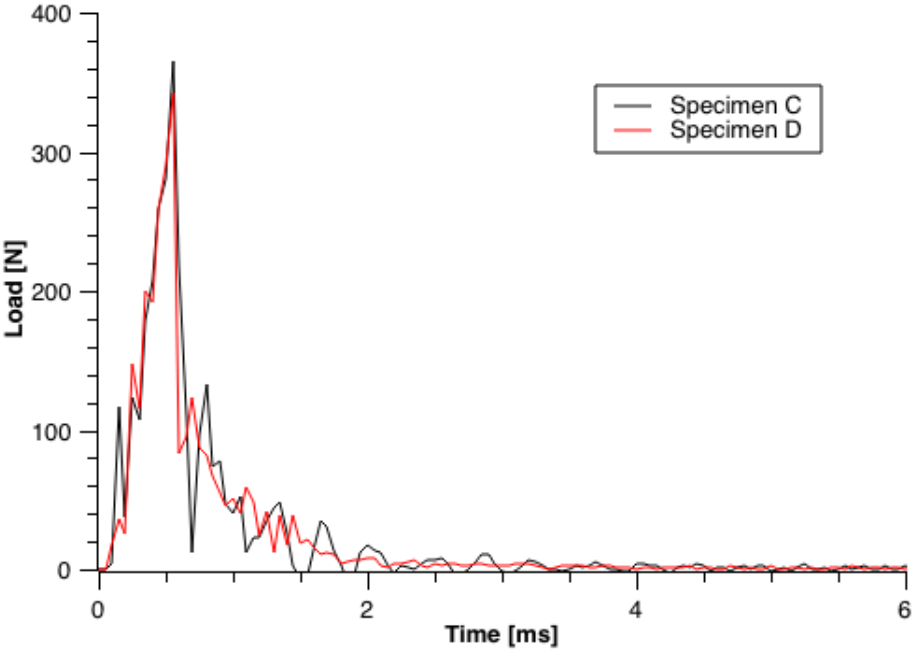

Figure 3.8: Results of the impact test performed on specimens C and D.

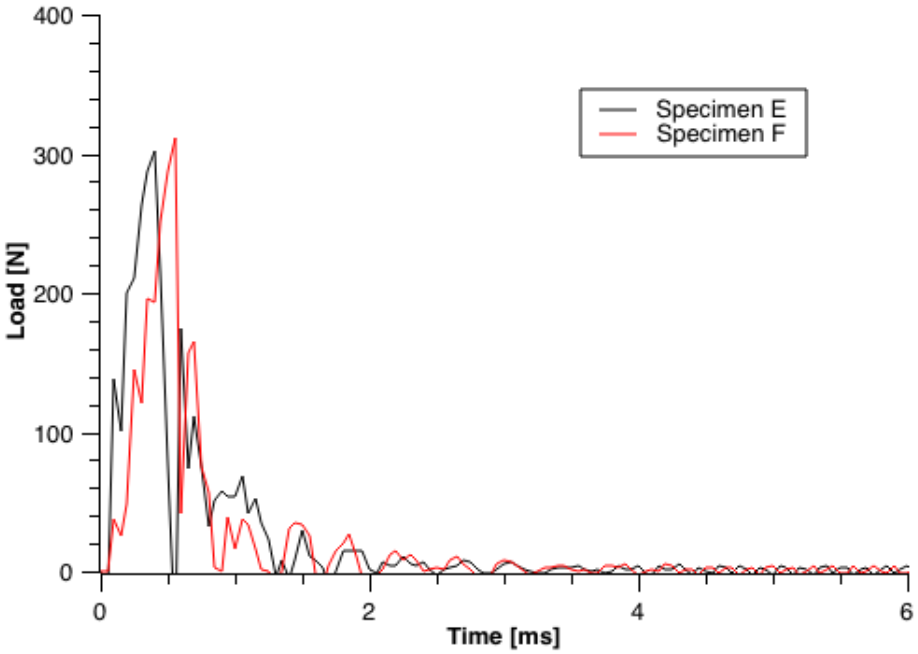

Figure 3.9: Results of the impact test performed on specimens E and F.

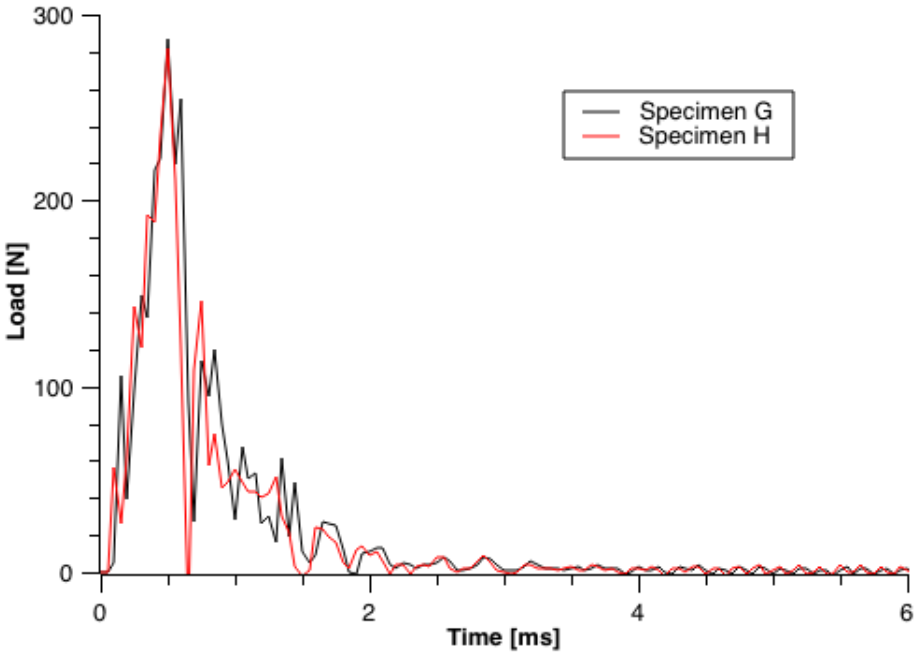

Figure 3.10: Results of the impact test performed on specimens G and H.

From the shape of the curves it is possible to notice that the material is relatively brittle with an applied load that reaches the maximum value rapidly and then decreases as well (but not immediately). In particular, it is possible to identify two portions of the curve; the one before the maximum peak is referring to the energy needed for the crack initiation while the part after the peak is related to the energy absorbed for the crack propagation.

The main results of the maximum load and specific absorbed energy calculations, obtained making reference to the load-displacement plots like that shown in Figure 3.11, are reported in Table 3.2 and showed graphically in Figure 3.12. As it is possible to see, the curve is characterised by peaks before the maximum one that are due to inertial effects, and peaks after the maximum one,

that are due to vibratory effects. In particular, for the calculation only the maximum peak must be considered.

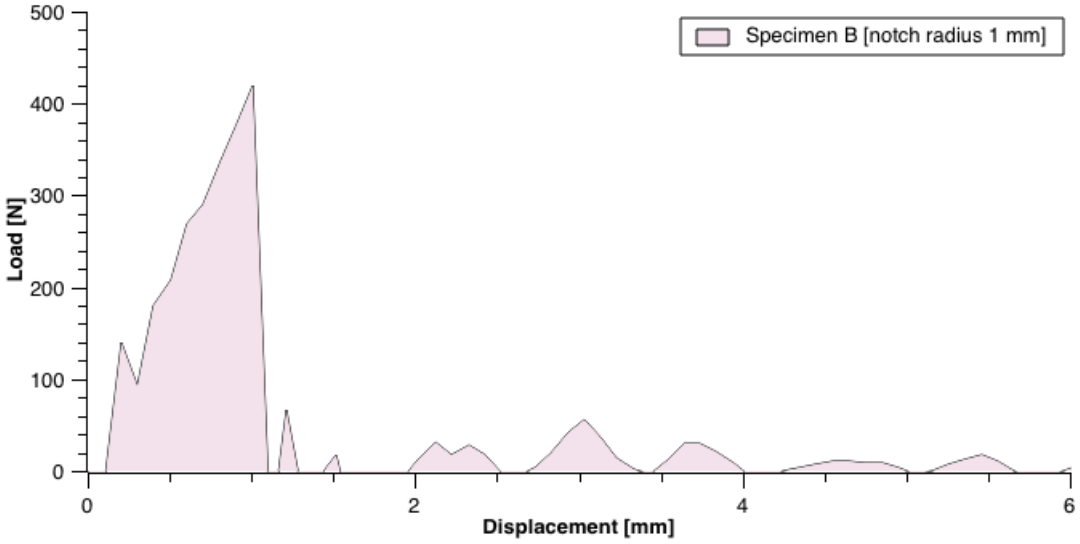

Figure 3.11: Example of load-displacement curve.

Specimens	Notch radius $[mm]$	Average F max $[N]$	Average specific absorbed energy $[kJ/m^2]$
A,B	1	403 ± 22	7.1 ± 0.5
C,D	0.25	354 ± 16	5.4 ± 1.1
E,F	0.10	306 ± 7	4.9 ± 0.6
G,H	0.01	286 ± 3	4.3 ± 0.2

Table 3.2: Maximum load and specific absorbed energy as functions of the notch radius.

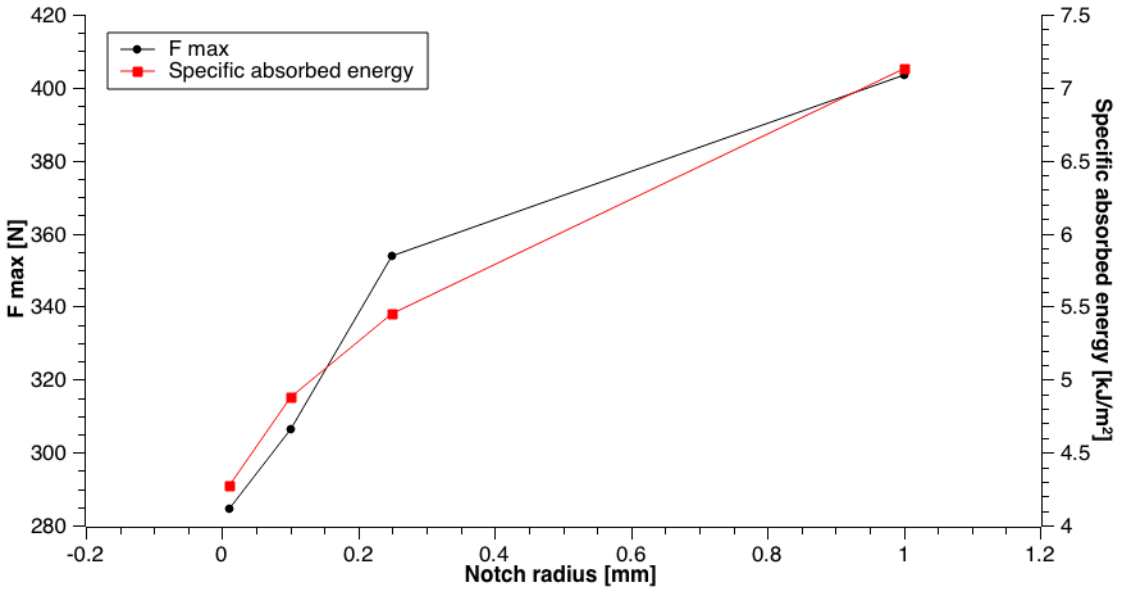

Figure 3.12: Notch radius dependence of average maximum load and maximum specific absorbed energy.

Considering the previous graphs and table it is possible to say that decreasing the notch radius the maximum force and the specific absorbed energy also decrease. This is due to the increase of the

stress intensification factor by reducing the radius of curvature of the notch tip. The reduction in the absorbed energy is a consequence of the lower maximum force needed to break the specimen.

4 Conclusions

The fracture toughness experiment yielded higher values of K_{IC} and G_{IC} for the specimens with smaller cross section, respectively of 5.5% and 4.4%. This may be due to the larger number of defects present in the volume of larger specimens. Due to the low sample size however a large error accompanied the calculated values. It is not clear whether the results are due to the underlying size effect phenomenon or simply a statistical error.

For what concerns the impact resistance analysis it is possible to say that a decrease in the notch radius of curvature corresponds to a more brittle behaviour of the material. The key point is the increase of the multiaxiality of the state of stress as the radius decrease and this produces an embrittlement of the material. In fact, passing from a radius of 1 *mm* to one of 0.01 *mm* the maximum force to break the specimen decreases from 403 ± 22 *N* to 286 ± 3 *N*. Correspondingly, the specific absorbed energy decreases from 7.1 ± 0.5 kJ/m^2 to 4.3 ± 0.2 kJ/m^2 as the radius decreases.

References

[1] T.R. Cuadrado,C.I. Vallo, P.E. Montemartini. *Effect of residual monomer content on some properties of a poly(methylmethacrylate)-based bone cement.* Journal of Applied Polymer Science, p.1367-1383, 1998.

[2] A. Martínez, A. Salazar, Noel Leon, Silvia Illescas, and Jesus Rodriguez. Influence of the notch-sharpening technique on styrene-acrylonitrile fracture behavior. *Journal of Applied Polymer Science*, 133, 05 2016.

[3] S. E. Barbosa,M. Etcheverry. *Glass Fiber Reinforced Polypropylene Mechanical Properties Enhancement by Adhesion Improvement*. Materials 5, p.1084-1113, 2012.

[4] R. Yahya ,R. A. Lafia-Araga ,N. A. Rahman, A. Hassan. *Impact Properties of Glass-fiber/Polypropylene Composites: The Influence of Fiber Loading, Specimen Geometry and Test Temperature*. Fibres and Polymers 14, p.1877-1885, 2013.

[5] *Standard Test Methods for Plane-Strain Fracture Toughness and Strain Energy Release Rate of Plastic Materials*. ASTM International, p.1-10, 2014.

[6] *Standard Test Method for Determining the Charpy Impact Resistance of Notched Specimens of Plastics*. ASTM International, p.1-17, 2008.